INCIDENT RADIATION AND THE ALLOCATION OF NITROGEN WITHIN ARCTIC PLANT CANOPIES; IMPLICATIONS FOR PREDICTING GROSS PRIMARY PRODUCTIVITY.

L. E. Street*[,1], G. R. Shaver[2], E.B. Rastetter[2], M. T. van Wijk[3,4], Kaye B. A.[2], M. Williams[1]

*Corresponding author
Email: l.e.street@ed-alumni.net
Telephone:+44 (0)131 650 6480
FAX: +44 (0) 131 662 0478
[1]School of GeoSciences
University of Edinburgh
Edinburgh, EH9 3JN, UK

[2]The Ecosystems Center
Marine Biological Laboratory
Woods Hole, MA 02543 USA

[3]Plant Production Systems,
Wageningen University,
Plant Sciences, Haarweg 333,
6709 RZ Wageningen, Netherlands.

[4]ILIRI, Sustainable Livestock Futures Group
P.O. Box 30709
Nairobi, Kenya

KEYWORDS: carbon balance, climate change, gross primary production, diffuse radiation, tundra vegetation, CO2 flux, specific leaf area, light extinction, nitrogen extinction

RUNNING TITLE: Arctic canopy N and primary productivity

ABSTRACT

Arctic vegetation is characterised by high spatial variability in plant functional type (PFT) composition and gross primary productivity (*P*). Despite this variability, the two main drivers of *P* in sub-Arctic tundra are leaf area index (L_T) and total foliar nitrogen (N_T). L_T and N_T have been shown to be tightly coupled across PFTs in sub-Arctic tundra vegetation, which simplifies up-scaling by allowing quantification of the main drivers of *P* from remotely sensed L_T. Our objective was to test the L_T-N_T relationship across multiple Arctic latitudes and to assess L_T as a predictor of gross primary productivity (*P*) for the pan-Arctic. Including PFT specific parameters in models of L_T-N_T coupling provided only incremental improvements in model fit, but significant improvements were gained from including site-specific parameters. The degree of curvature in the L_T-N_T relationship, controlled by a fitted canopy nitrogen extinction co-efficient, was negatively related to average levels of diffuse radiation at a site. This is consistent with theoretical predictions of more uniform vertical canopy N distributions under diffuse light conditions. Higher latitude sites had higher average leaf N content by mass (N_M), and we show for the first time that L_T-N_T coupling is achieved across latitudes via *canopy scale* trade-offs between N_M and leaf mass per unit leaf area (L_M). Site-specific parameters provided small but significant improvements in models of *P* based on L_T and moss cover. Our results suggest that differences in L_T-N_T coupling between sites could be used to improve pan-Arctic models of *P* and we provide unique evidence that prevailing radiation conditions can significantly affect N allocation over regional scales.

INTRODUCTION

Photosynthetic CO_2 uptake by vegetation, gross primary productivity (*P*), is a key component of the carbon cycle and is strongly linked to climate conditions (Beer *et al.*, 2010). The impacts of climate change on *P* are a major research topic (Piao *et al.*, 2007, Reichstein *et al.*, 2007, Falge *et al.*, 2002, Ziehn *et al.*, 2011). The Arctic climate is warming more quickly than elsewhere on the globe (Bekryaev *et al.*, 2010) and by accelerating nutrient mineralisation in soils, is expected to drive increases in Arctic plant productivity (Hill *et al.*, 2011, Grant *et al.*, 2011, Chapin *et al.*, 1995). Arctic terrestrial carbon stocks are large, 98 Pg in North American Arctic soils alone (Ping *et al.*, 2008), so there is a pressing need to understand terrestrial Arctic C balance in order to quantify carbon cycle – climate feedbacks. This requires robust estimation and prediction of *P* over pan-Arctic scales.

Quantification and prediction of *P* is complicated by high spatial and temporal variability (Williams *et al.*, 1999, Street *et al.*, 2007). One approach to extrapolating across space and time uses process-orientated models which can incorporate remotely sensed information on the spatial and temporal drivers of *P* (Ryu *et al.*, 2011, Sitch *et al.*, 2007). These drivers include light intensity and temperature, as well as plant biomass or leaf area index (m^2 of leaf per m^2 ground). Process-based models of *P* are based on well-understood biochemical processes at the leaf level (Collatz *et al.*, 1992, Farquhar *et al.*, 1980, von Caemmerer *et al.*, 1981) which must be scaled to whole plant canopies. Up-scaling from leaf to canopy is challenging because photosynthesis responds non-linearly to light, and non-linear gradients of light intensity and leaf properties occur within canopies (de Pury *et al.*, 1997, Leuning *et al.*, 1995). Many current models are based on optimization theory (Clark *et al.*, 2011, Ryu *et al.*, 2011) which states that photosynthesis is optimised if leaf-level nitrogen concentration per unit leaf area (N_L), which is

directly related to photosynthetic capacity, (Evans, 1989) varies in proportion to vertical light gradients (Field, 1983, Hirose *et al.*, 1987, Hikosaka *et al.*, 1998). However, radiative transfer within canopies in turn depends on structural characteristics such as canopy height, leaf clumping, and leaf angle distribution (Niinemets, 2010, Hikosaka *et al.*, 1997), as well as the amount of diffuse versus direct radiation (Roderick *et al.*, 2001). Canopy structural properties vary between species and plant functional types (Anten *et al.*, 1999, Anten *et al.*, 1995) and the properties of leaves themselves, including the maximum photosynthetic capacity, vary considerably both within and between species (Wright *et al.*, 2004).

Previous studies in low Arctic shrub and tussock tundra ecosystems (in N. Sweden and N. Alaska) suggest however, that there are unexpected system level interactions within mixed species plant canopies which can simplify variability in leaf properties and canopy structure at the stand scale. Van Wijk *et al.* (2005) and Williams & Rastetter (1999) show that per unit ground area, the total leaf nitrogen (N_T) of plant canopies follows a tightly constrained relationship with L_T across a range of PFTs, despite large variation in N_L at the species level. Average *canopy* foliar nitrogen concentration per unit leaf area (N_T/L_T) was1.9 g N m^{-2} across a wide range of vegetation types when $L_T < 1.0$ m^2 m^{-2}. Crucially, they show that the variability in N_T/L_T was less than would be expected if canopies were randomly constructed from the pool of available species, suggesting convergence of leaf-level properties at the canopy scale, rather than a central tendency towards the mean value of N_L.

L_T and N_T have also been shown to be the most important drivers of P in Swedish and Alaskan tundra; a strong correlation between L_T (determining light capture) and N_T (determining light utilisation by photosynthetic enzymes) optimising P by balancing limitations on photosynthesis (Williams *et al.*, 1999). This has been confirmed in plot scales studies in which

L_T alone explained 80 % of the variability in P at constant light level (Shaver *et al.*, 2007, Street *et al.*, 2007). The tight coupling between L_T, N_T and P greatly simplifies up-scaling, by reducing species level variability, and allowing remote-sensed estimates of P based on L_T or N_T alone. Whether the canopy-scale relationship between L_T and N_T in Sweden and Alaska, and the corresponding linkages to P, are general ecological scaling relationships applicable across the pan-Arctic has not previously been tested. To address this, we ask the following questions: 1) is there a general relationship between L_T and N_T for Arctic vegetation? and 2) is there a general relationship between P and L_T across the Arctic?

While soil nutrient availability may dictate patterns of plant abundance and therefore L_T (Shaver *et al.*, 1980, Shaver *et al.*, 1986, 1991), we expect that lower irradiance at higher latitudes will modify the optimal development of leaf area with respect to available nitrogen; L_T-N_T will be coupled but shifted towards lower N_T per unit leaf area. We expect lower N_T per unit leaf area to result in lower P per unit leaf area, under saturating light conditions. To test these hypotheses, we present destructive measurements of N_T and L_T across five Arctic sites spanning latitudes from 68 – 78 ºN. We compare fitted relationships between N_T and L_T to patterns of incident radiation; both total short-wave (SW) radiation and the SW diffuse fraction. We use 1 m × 1 m chamber measurements of P, together with indirect measurements of L_T based on the normalised difference vegetation index (NDVI), to explore the relationship between L_T and P.

MATERIALS AND METHODS

A list of symbols and abbreviations is given in Table 1. The present analysis combines new N_T, L_T, and P data from near Longyearbyen, Svalbard, from Zackenberg, NE Greenland, and from Barrow, Alaska with previously published data from Abisko, northern Sweden and from near Toolik Lake, Alaska (Table 2). We measured L_T and N_T destructively on small (0.03 – 0.09 m^2) harvest plots (Table 2). We measure CO_2 fluxes on different (1 m^2) flux plots. We used NDVI to estimate L_T for the 1m^2 flux plots using site-specific calibrations between L_T and NDVI based on the smaller harvested plots. To improve the performance of these calibration relationships we also include moss % cover as an explanatory variable in the L_T-NDVI model. We used NDVI to measure L_T for the flux plots because 1) it is non-destructive and 2) it allows for measurement of L_T on larger scales (1m^2 harvests would not have been feasible). The use of NDVI to measure L_T also increases the relevance of the analysis for up-scaling, though comparing hand-held NDVI measurements to satellite derived values is beyond the scope of this study.

Site descriptions

LONGYEARBYEN, SVALBARD

We measured CO_2 flux using chamber techniques and sampled vegetation at ten sub-sites, all within approximately 20 km of the town of Longyearbyen, on the island of Spitzbergen (78° 13'N, 15°37'E). Mean annual air temperature (MAT) for Longyearbyen is -5 °C, mean July temperature is 6°C and mean precipitation ~310mm (Forland *et al.*, 2000). Vegetation in the fjord (Adventdalen) in which Longyearbyen is situated ranges from salt marsh on the margins of the estuary, to wet sedge meadow (mostly *Dupontia*, *Carex* and *Eriophorum spp.*) on the flat valley bottom, to dwarf shrub heath communities on well drained slopes. Dwarf shrub vegetation

is characterized by locally dominant patches of *Cassiope tetragona*, *Dryas octopetala*, and *Salix polaris* communities (Baddeley *et al.*, 1994). Plots were chosen to sample the range of vegetation types within the area. All field measurements were made 14th July - 3rd August 2005.

ZACKENBERG, GREENLAND

We measured CO_2 flux using chamber techniques and sampled vegetation at sub-sites within approximately 2 km of Zackenberg Research Station (74° 28'N, 20°34'E) and below an elevation of 100 m. Mean annual air temperature (1996 – 2008) for Zackenberg, is –9.0 °C, mean July temperature is 6.1 °C, with a total annual precipitation of 218 mm (www.zackenberg.dk). Vegetation in the area around Zackenberg consists of wet fen and grassland in areas by water tracks, with heath vegetation dominated by *Cassiope tetragona* on better drained level ground. Heath dominated by *Vaccinium uliginosum* or *Dryas* species is more common on exposed slopes. There are also extensive areas of snowbed vegetation dominated by *Salix arctica*. Plots were chosen to sample the range of vegetation types within the area. All field measurements were made between 8th July – 1st August 2006.

BARROW, ALASKA

Flux measurements, leaf harvests, and reflectance measurements were made in the Barrow Environmental Observatory (BEO) near Barrow, Alaska (71°18′N, 156°40′W) in July 2009. All measurements were made within a single, shallow, drained and revegetated thaw lake basin and surrounding shoreline ridges. The area was entirely underlain by permafrost with ice-wedge polygons creating local microrelief. Sites were selected to represent vegetation along a soil moisture gradient, from constantly-flooded, emergent wet-sedge vegetation dominated by

rhizomatous sedges and grasses to relatively dry ridges dominated by creeping willow species and grasses. Vegetation, soils, and climate in the Barrow region have been thoroughly described in past research (Brown *et al.*, 1980), including at the BEO adjacent to sites used in this research (Hollister *et al.*, 2005). Annual temperature at Barrow is -11 °C and the long-term average temperature in July is 4 °C although this has increased in recent decades.

Abisko, Sweden

We used leaf harvest data from near Abisko in Northern Sweden (68°18′N,18°51′E) collected between the 15th July and 30th July 2002 (van Wijk *et al.*, 2005). We use CO_2 flux data collected between the 22nd July and 5th August 2004 at two sites nearby the site of vegetation sampling, (the 'Stepps' site and 'Paddus' site), and at another upland site (the 'Latnja' site) (Shaver *et al.*, 2007). MAT at Abisko is -1 °C, mean July temperature is 11 °C and mean annual precipitation is 225-475 mm (van Wijk *et al.*, 2005).

Toolik, Alaska

We used L_T and N_T data collected during 1997 as part of the Arctic flux study within the Kuparuk watershed on the northern side of the Brooks Range, AK, USA (Williams *et al.*, 1999). We use CO_2 flux data collected between 12th July and 4th August 2004 in tussock, dry heath and shrub tundra at Toolik Lake (68º38'N,149º36'W) and nearby at Imnavait Creek (68º37'N,149º19'W) (Shaver *et al.*, 2007). Though at the same latitude as Abisko, the climate at

Toolik is more continental; MAT at Toolik Lake is -10 °C and mean July temperature is 14 °C. Mean annual precipitation is 200-400 mm (van Wijk *et al.*, 2005).

Measurements

NDVI, LEAF AREA INDEX AND CANOPY N OF HARVEST PLOTS

We measured L_T, N_T, and total leaf biomass (M_T) of harvested plots at Svalbard (n = 48) , Zackenberg (n = 78), Barrow (n = 23), Toolik (n = 92) and Abisko (n = 94) . The size of the harvested plots was between 0.03 and 0.09 m^2 (Table 2). At Zackenberg, Svalbard, and Barrow we also measured the NDVI of each plot before harvesting using a Unispec spectral analyser (PP systems, Haverhill, Massachusetts, USA) following the methods of Street *et al.* (2007). The Unispec instrument records reflectance spectra from 0.3 mm to 1.0 mm. We held the sensor at a vertical height (< 1m) such that the field of view equated to the area being harvested (Table 2). The sensor was positioned over the plot using a 1m ruler held vertically in the centre of the plot; the ruler was removed prior to measurement. We calculated NDVI using the formula:

$$NDVI = (R_{NIR} - R_{VIS})/(R_{NIR} + R_{VIS})$$

where R_{NIR} is reflectance at a wavelength of 0.725–1.0 μm and R_{VIS} is reflectance at 0.56–0.68 μm. Reflected radiation was calculated as a proportion of incident radiation using a standard white (barium sulphate) reference panel. Reference panel readings were taken prior to each measurement. The NDVI of the surface was also measured after the canopy was removed ($NDVI_{post}$), within 1 hour of the top of canopy measurement. NDVI measurements were generally made between 10 am and 4 pm.

L_T, M_T and N_T were measured destructively, following the methods of Van Wijk *et al.* (2005). For *Cassiope tetragona* we doubled the one-sided projected leaf area (Campioli *et al.*,

2009b). We estimated the percent cover of bryophytes for each plot, and at Svalbard and Zackenberg re-measured NDVI following removal of the vascular plant canopy.

NDVI, LEAF AREA INDEX AND PERCENT COVER OF FLUX PLOTS

We measured the NDVI of flux plots in Svalbard, Barrow and Zackenberg using the Unispec analyser in a grid of 9 points, following the methods of Street *et. al.* (2007). We estimated absolute aerial cover in each flux plot for all vascular plants by species (i.e. total cover can be > 100%), and for bryophytes. We did this by placing a 5 × 5 string grid (each square = 0.04 m^2) over the plot, and visually estimating cover in each square, then calculated an average species cover for the entire plot. Both harvest and flux plots were classified as either deciduous, evergreen, graminoid or mixed vegetation according to the contribution of each functional type to total biomass (for the harvest plots) or cover (for the flux plots). Plots with the abundance of a single PFT > 70 % were classified as that type, otherwise plots were classified as mixed.

To estimate L_T for the flux plots from NDVI we used calibration relationships between NDVI and L_T for each plant functional type based on destructive data from the harvested plots. We modelled the relationship between L_T and NDVI using an equation modified from Steltzer & Welker (2006):

$$L_T = \frac{1}{Kc} \ln\left(\frac{NDVI_{\min} - NDVI_{\max}}{NDVI - NDVI_{\max}} \right) \quad (1)$$

Where $NDVI_{max}$ is a fitted parameter representing the theoretical maximum possible NDVI for a vegetation canopy (which cannot be measured for open high Arctic canopies) and K_c is a fitted extinction co-efficient. $NDVI_{min}$ is a parameter representing the minimum possible NDVI of the

background surface (i.e. soil or moss). We used the minimum measured value of $NDVI_{post}$ (0.24) as an estimate of $NDVI_{min}$ when fitting equation 1.

To take into account the effect of mosses on NDVI, and therefore potentially improve the accuracy of our L_T estimates, we also fitted a second model in which we assume that $NDVI_{min}$ increases as moss cover increases. In other words, the ground surface underneath the vascular canopy on average becomes greener as mosses become more abundant, but at any moss cover there is still a distribution of possible background NDVI values - the minimum of which representing $NDVI_{min}$. We observed a significant correlation between bryophyte cover and $NDVI_{post}$, as shown in Figure 1 so we used the slope of this relationship (0.0024 $\%^{-1}$) as an estimate of the rate of increase in $NDVI_{min}$ as moss cover increases (*a* in equation 2).

$$L_T = \frac{1}{Kc}\ln\left(\frac{\left[aB_c + 0.24\right] - NDVI_{max}}{NDVI - NDVI_{max}}\right) \quad (2)$$

Where B_c is bryophyte cover (%). Note that there are two fitted parameters in both equation 1 and 2.

For both Toolik and Alaska we used the previously published values of L_T for each flux measurement plot, based on vegetation specific NDVI - L_T calibrations (Street *et al.*, 2007).

Flux measurements

We measured the light response of net ecosystem CO_2 exchange (F_c), and ecosystem respiration (R_E) in Svalbard, Zackenberg, Barrow, Toolik and Abisko over 1 × 1 m patches of vegetation (Table 2). All flux measurements were made using protocols described in Williams *et al.* (2006) , Street *et al*. (2007) and Shaver *et al.* (2007). In Zackenberg we also measured fluxes for 15 0.3 m

× 0.3 m patches using a smaller chamber and destructively sampled L_T. For the Toolik and Abisko CO_2 flux data we used a sub-set of the data presented in Shaver *et al.* (2007) that coincided with the dates of CO_2 flux data collection at other sites (July – early August).

Data analysis

LAI and total canopy N

We aimed to find the parameters for a theoretical model that relates N_T to L_T – and to determine whether the parameters describing the model differ significantly between sites. It has been argued that an exponential decline in foliar N through the canopy is a plant strategy for maximizing canopy photosynthesis with respect to canopy nitrogen (Field, 1983, Hirose *et al.*, 1987, Hikosaka *et al.*, 1998).

$$N_L = N_0 e^{-\gamma L_c} \quad (3)$$

where N_L is the nitrogen concentration of a leaf in the canopy (g N m^{-2} leaf), N_0 is the top of the canopy nitrogen concentration (g N m^{-2} leaf), γ an extinction coefficient (m^2 ground m^{-2} leaf), and L_c is the cumulative leaf area above the leaf (m^2 leaf m^{-2}ground). Total canopy nitrogen is then the integral of equation 3.

$$N_T = \int_0^{L_T} (N)\, d\, L = \frac{N_0}{\gamma}\left(1 - e^{-\gamma L_T}\right) \quad (4)$$

where N_T is the total canopy nitrogen (g N m^{-2} ground) and L_T is leaf area index (m^2 leaf m^{-2}ground). Equation 4 would be expected to describe the relationship between N_T and L_T if N_0 and γ are uniform over the area sampled.

CO_2 flux

To test the relationship between L_T and canopy photosynthesis, we compare the parameters of fitted *P* light response curves to L_T for each 1 × 1 m plot. *P* at each light level was calculated by subtracting F_c from R_E. The light response of photosynthesis was then modelled with a rectangular hyperbola

$$P = \frac{P_{max} \times I}{\left(\frac{P_{max}}{E_0}\right) + I} \quad (5)$$

where P_{max} is the rate of light saturated canopy level photosynthesis (μmol CO_2 m^{-2} s^{-1}), *I* is the incident photosynthetic flux density (μmol photons m^{-2} s^{-1}), E_0 is the initial slope of the light response curve or canopy-level quantum efficiency at low light levels (μmol CO_2 μmol^{-1} photons).

Each light curve was used to predict *P* at 1000 μmol photons m^{-2} s^{-1} (P_{1000}). We compared the relationship between *P* near light saturation (P_{1000}) and leaf area, using only curves where maximum *I* measured during the light curve exceeded 1000 μmol photons m^{-2} s^{-1}. We assume leaf level photosynthesis at 1000 μmol^{-1} photons (P_{1000}) is approximately linearly related to N_L (Hirose and Werger 1987) and therefore follows an exponential distribution with canopy depth as N_L, giving an analogous equation to equation 4 but with a constant term for moss photosynthesis :

$$P_{1000} = \frac{P_0}{\gamma_p}\left(1 - e^{-\gamma_p LAI}\right) + P_m \quad (6)$$

where P_{1000} is canopy-level gross photosynthesis at 1000 μmol photons m^{-2} s^{-1}, P_0 is top of the canopy P per unit leaf area at 1000, γ_p is the extinction of leaf level P with canopy depth and P_m is a constant term for moss photosynthesis.

We also compare the relationship between canopy-level quantum efficiency E_0 (the initial slope of the light response curve, equation 5) and L_T. We assume that E_0 is not strongly related to leaf N concentration at low light levels (Hirose and Werger 1987) and therefore follows a uniform distribution through the canopy and a linear relationship with L_T. We again include a constant for the photosynthetic activity of mosses:

$$E_0 = \alpha.LAI + E_m \quad (7)$$

Where E_0 is canopy-level quantum efficiency at low light levels (μmol CO_2 μmol^{-1} photons), α is the increase in E_0 per unit canopy leaf area, and E_m is a constant representing photosynthetic activity of mosses.

Statistical analysis

We compared alternate statistical models of the relationship between N_T and L_T (equation 4), P_{1000} and L_T (equation 6) and E_0 and L_T (equation 7) using general non-linear least squares fitting procedures in the 'nlme' library for R Version 2.12.1 (R Development Core Team (2008)). We initially fit a general model to the whole data set. We then repeated the model fitting including site (or PFT) based groupings for the data, both for individual parameters and parameters in combination. For example, for the N_T model (equation 4) we compared the general model to

alternate models that included 1) site-specific fitted values of N_0 with a general fitted value for γ, 2) site-specific fitted values of γ with a general fitted value for N_0 and 3) site-specific fitted values of both N_0 and γ. We then repeated the analysis using PFT instead of site to group the data. We do not show results for models with PFT specific values of N_0 or γ alone, as even with PFT effects for both parameters, we saw little improvement in model fit. For the P_{1000} and E_0 models we also show results for a restricted set of possible data groupings because improvements in model fit by grouping the data by PFT were small. Alternative models were compared using Akaike's Information Criterion (AIC), Bayes Information Criterion (BIC), loglikelihood (LogLik) ratio tests and the root mean square error (RMSE) of model predictions. We included power variance functions in all N_T models, to account for heteroscedasticity in the data. It was necessary to include power variance functions to account for heteroscedasticity in the E_0 data, but not in the P_{1000} data.

Radiation data

To investigate the effect of the radiation environment, we compared site-specific fitted parameters for equation 4 to average solar radiation conditions. We used 5 years of data for which we were able to obtain continuous data for every site (1998-2000, 2003 & 2005). We calculated the sum of hourly short-wave (SW) radiation over the growing season (defined as 1st June to 31st August) for each year, then calculated the mean and standard deviation across years for each site. We calculated the average diffuse radiation fraction by averaging hourly daytime (defined as the period where incident SW > 20 Wm^{-2} or approximately 40 $\mu mol\ m^{-2}\ s^{-1}$ I) diffuse fraction over each growing season. For Svalbard we used hourly global SW and diffuse SW data from Ny-Alesund, approximately 100 km NW of Longyearbyen (supplied by the Alfred-Wegner

Institute, www.awi.de). For Abisko we used hourly global SW data provided by Abisko Scientific Research Station (www.ans.kiruna.se) to model hourly diffuse SW fraction based on the ratio of modelled extraterrestrial to measured global SW according to Erbs *et al.* (1982). We tested the Erbs model with 2.5 weeks of global and diffuse SW data provided by the ABACUS project (www.geos.ed.ac.uk/abacus). For Toolik we used global SW data from the Toolik Lake Long Term Ecological Research (LTER) database (ecosystems.mbl.edu/ARC) to model daily diffuse SW fraction. We tested the Erbs model results at Toolik with 6 weeks of total and diffuse *I* from late summer 2008 provided by the Arctic Observing Network (aon.iab.uaf.edu). Global SW was estimated from *I* using an empirical relationship for that site (see Supplementary Material). For Zackenberg we used hourly global SW data provided by the ClimateBasis programme at Zackenberg research station (available at www.zackenberg.dk/data/). For Barrow we use measured SW and diffuse SW data provided by the US Atmospheric Radiation Monitoring program (ARM) (www.arm.gov).

RESULTS

Leaf area index and total foliar nitrogen

L_T was < 1.0 m^2 m^{-2} in 90 % of the 151 harvests carried out at Zackenberg, Svalbard and Barrow reflecting the characteristic short stature, low L_T plant canopies at higher latitude and coastal tundra vegetation compared to lower latitudes. The maximum N_T values recorded (across all sites) were in Svalbard with ~ 4.5 g N m^{-2} ground (Fig. 2b). Relationships between N_T and total leaf mass (M_T, g leaf m^{-2} ground area), and between L_T and M_T were less well-constrained than the relationship between L_T and N_T both within and across sites (Fig. 2 a b & c, Fig. 3). Canopies with low average N concentration per unit leaf mass, (N_T/M_T) tended to have greater average leaf

mass per area (M_T/L_T) (Fig 2d). The highest average canopy N_T/M_T values were in Zackenberg; which in several plots was > 35 mg N g^{-1} leaf (Fig 2d). At L_T <1, average N_T/M_T at each site was greater at Zackenberg (25.8 ± 1.1 mg N g^{-1} leaf), Svalbard (21.4 ± 0.8 mg N g^{-1} leaf) and Barrow (24.8 ± 0.8 mg N g^{-1} leaf) than at the lower latitude sites Toolik (18.8 ± 0.4 mg N g^{-1} leaf) and Abisko (12.1 ± 0.5 mg N g^{-1} leaf).

Average leaf-level nitrogen concentrations by mass for individual species (N_M) varied between 16 mg N g^{-1} (1.6 % by mass) in *Dryas* leaves at Zackenberg, and 38 mg N g^{-1} (3.8 % by mass) in *Polygonum viviparum* at Zackenberg. Nitrogen concentrations per unit leaf area (N_L) for individual species varied > 4-fold, from 0.95 g N m^{-2} for *Saxifraga cernua* at Barrow, to > 4.0 g N m^{-2} in forbs and graminoids at Zackenberg (Table 3).

Including site specific parameters in the N_T model (equation 4) resulted in significant improvements in model fit compared to the general model (Table 4). The lowest RMSE (0.18 g N m^{-2}) was achieved by including site specific parameters both for N_0 and γ, with significantly improvements in fit (assessed with Loglikelihood ratio tests) both over the general model, and models with site specific fitted parameters for either N_0 or γ alone (Table 4). The overall R^2 of modelled versus measured values for a model with site specific N_0 and γ was 0.93. The average site-specific fitted value for top of canopy nitrogen concentration (N_0) was 2.2 g N m^{-2}, with a standard deviation of 0.2 g N m^{-2}, or coefficient of variation (CV) of 9 %. The average site-specific fitted extinction coefficient, γ, was 0.22, with standard deviation across sites of 0.31 or CV of 140 %.

Including PFT specific parameters in the N_T model also resulted in a significant improvement in model fit, but the reduction in RMSE (from 0.27 to 0.25 g N m^{-2}) and associated increase in LogLiklihood were small compared to the site specific models (Table 4).

Radiation conditions

Total growing season SW radiation was lowest for Svalbard at 1310 ± 100 MJ m^{-2} (1 S.D) and greatest at Zackenberg at 1707 ± 111 MJ m^{-2} (1 S.D) (Fig. 4a.). The Erbs *et al.* (1982) model of diffuse radiation fraction performed well when tested with measured data from Abisko (Supp. Material Fig. 2 a & b) though there was a slight bias (daily modelled vs. measured diffuse radiation slope = 1.11, intercept = -0.59, R^2 = 0.86, RMSE = 0.99 MJ m^{-2} day^{-1}). This bias was corrected for when calculating average growing season diffuse fraction. We also corrected for bias at Toolik Lake (daily modelled vs. measured diffuse radiation slope = 1.02, intercept = 0.69, R^2 = 0.72, RMSE = 1.38 MJ m^{-2} day^{-1}). The average diffuse fraction was greatest in Svalbard (80 % ± 3.5 % (1 S.D.)) and lowest at Zackenberg (62 % ± 3.9 % (1 S.D.)). There was a positive trend in site specific fitted values of N_0 with total growing season radiation, which was not statistically significant (Fig 4a). There was a significant negative trend in site specific fitted values of γ with increasing diffuse radiation fraction (Fig. 4b) (P = 0.018).

Leaf area index and NDVI

We found a significant positive correlation between $NDVI_{post}$ and B_c (Spearman ρ = 0.73, $p < 0.001$). NDVI for ground with < 10 % moss cover was 0.38 ± 0.0057 (1 SE), for ground with > 90 % moss cover NDVI was 0.61 ± 0.0028 (1 SE). The slope of the linear relationship (least-squares fit) between $NDVI_{post}$ and % moss cover was 0.0024 $\%^{-1}$ (Fig 1). There was a clear relationship between NDVI and observed L_T in Svalbard, for plots with both low and high moss cover (Fig 5a). The relationship between L_T and NDVI was more scattered for Zackenberg, with a clustering of points with > 50 % moss cover at high NDVI values but low L_T values (Fig 5c).

Including moss cover as an explanatory variable in the L_T-NDVI model (equation 2), parameterised separately for each PFT, we could explain 74 % of the variation in L_T at Svalbard (Fig 5b). If we did not include the effect of mosses on NDVI (i.e. by using equation 1) in the PFT specific calibrations, we could explain 70 %. Likewise for Zackenberg, we could explain 49 % of the variation in L_T using equation 2 (Fig 5d), but with equation 1 we could explain 37 %. Data from Barrow were limited so we parameterised the L_T -NDVI relationship for graminoids, and combined mixed/forb and deciduous vegetation. We could explain 34 % of the variation in L_T at Barrow using equation 2 (Fig 5f); NDVI alone (equation 1) explained 23 %. The NDVI calibration relationships used to predict L_T for Abisko and Toolik, published in Street *et. al*. 2007, explained 84 % of the variation in L_T.

Leaf area index and canopy photosynthesis

P_{1000} increased with L_T for all sites, up to a maximum value of 17 μmol m^{-2} s^{-1}. The flux plots at Toolik and Abisko had greater L_T than the higher latitude sites, up to 2 m^2 m^{-2}, and also had the highest values of P_{1000} (Figure 6a). There was a large degree of overlap in the relationship between P_{1000} and L_T between sites (Figure 6a). Fitted P_0 for the general P_{1000} model (equation 6) was 11.8 μmol m^{-2} s^{-1} and γ_p was 0.6 m^{-2} ground m^{-2} leaf. Including site effects in the model resulted in significant but small increases in model fit over the general model (Table 5). The fitting routine was unable to find a solution with site-specific fitted parameters for P_0, γ_P and P_m indicating model over-parameterisation. Fitting equation 6 with site specific parameters for γ_P and P_m gave the best model fit, and resulted in a reduction in RMSE from 1.89 to 1.71 μmol m^{-2} s^{-1}, with a modelled vs. measured R^2 of 0.78. Including PFT specific fitted parameters for γ_P and P_m, and P_0 and γ_P resulted in small improvements in RMSE, but increased the AIC and resulted

in insignificant Loglikelihood ratio tests compared to the general model; indicating that the data do not provide support for a PFT specific model.

E_0 also increased with increasing L_T and had a maximum value of 0.047 μmol CO_2 μmol^{-1} photons (Figure 6b). There was also a high degree of overlap between sites in Figure 6b, and we found no significant improvements in model fit by including site or PFT specific parameters in the E_0 model (equation 7). The general model was associated with the lowest AIC value and had slope of 0.017 μmol CO_2 μmol^{-1} photons m^{-2} and intercept of 0.005 μmol CO_2 μmol^{-1} photons. R^2 of the linear regression between modelled and measured values was 0.67.

DISCUSSION

Is there a pan-Arctic relationship between leaf area index and total foliar nitrogen?

The fit of the N_T model was only marginally improved by including PFT specific parameterisations, consistent with the conclusions of Van Wijk *et al.* (2005) and Campioli *et al.* (2009a) that the relationship between L_T and N_T converges for a wide range of vegetation types. Including site-specific parameters led to much greater improvements in model fit. Our cross-site estimate of 2.2 g N m^{-2} for N_0 is close to the average canopy N_T/L_T of 1.9 g N m^{-2} reported by Van Wijk *et al* (2005) for Abisko and Toolik. Contrary to our original hypothesis we found no evidence that the L_T-N_T relationship is shifted towards lower N per unit leaf area at higher latitude. Values of N_0, representing top of canopy N per unit leaf area, were highest at Zackenberg, the second most northerly site. There was also no latitudinal pattern in the fitted parameter for the curvature of the relationship (γ).

The large variability (large CV) in fitted γ compared to N_0 is reflected by the divergence between sites in Fig 2b, which increases as L_T increases; there is a large degree of overlap at low L_T. The convergence in the N_T-L_T relationship at low L_T occurs despite large variation in average canopy foliar N concentration by mass (N_T/M_T) and leaf thickness (L_T/M_T) *between* as well as *within* sites. For example, average N_T/M_T at Zackenberg, Svalbard and Barrow was greater than at Toolik and Abisko. Higher metabolite concentrations in colder climates can be expected as an acclimation response to lower rates of enzyme activity (Chapin *et al.*, 1983), or because of passive lack of dilution resulting from slower growth (Weih *et al.*, 2001). Alternatively, the shorter growing season in Svalbard and Zackenberg may favour short-lived leaves, which tend to be thinner (Shipley *et al.*, 2006) forcing canopies to concentrate N per unit mass. There are therefore site level difference in the way L_T-N_T coupling is achieved; in Svalbard and

Zackenberg leaves are thinner with higher N concentration by mass (*Cassiope tetragona*, the only abundant evergreen shrub, being the exception), whereas in Sweden, leaves tend to be thicker, with lower N concentration by mass. This is reflected in the clustering of points along the length of the curve shown in Fig 2d. Trade-offs between leaf properties have been well documented across species at the global scale (Wright *et al.*, 2004, Reich *et al.*, 2004). This is the first time such trade-offs have been documented as an 'emergent' system-level property of mixed species plant canopies.

The influence of radiation

Our data suggest that radiation conditions have an impact on N allocation, but that this is not a direct result of changes in latitude and therefore day-length and/or sun angle. We demonstrate a significant correlation between L_T-N_T curvature (γ) and fraction diffuse SW (Fig. 4b). While not proof of a causal link, this finding is consistent with theory (Hirose, 2005, Niinemets, 2007) which suggests that canopy N is allocated optimally if N_L declines in proportion to light extinction with canopy depth. Measured gradients in leaf N content in the field are often sub-optimal (Meir *et al.*, 2002, Bond *et al.*, 1999); the degree of N extinction is less than would maximise potential carbon gain. Nevertheless, it follows that under diffuse conditions *N* should be distributed more uniformly due to greater light penetration into the canopy (Roderick *et al.*, 2001, Meir *et al.*, 2002). There are other important influences on canopy light penetration, such as canopy height, leaf angle and geometry (Anten *et al.*, 1995) but the lack of significant improvements in model fit when incorporating PFT specific parameters suggests that the properties of incident radiation may be more important in controlling the distribution of N.

Differences in diffuse radiation between sites can be explained by differences in cloudiness. Zackenberg had the lowest average summer diffuse fraction, and Svalbard the highest. Remotely sensed maps of cloud frequency (Wylie *et al.*, 2005) show high cloud cover (approaching 100%) over the polar oceans and around Svalbard. Cloud frequency over Greenland is lower (around 60 %) than that of terrestrial Arctic at lower latitudes presumably because of the influence of the Greenland ice cap on cloud formation. Low cloud frequency at Zackenberg also explains how the total incident SW radiation can be greater than at lower latitude sites (Fig 4a.).

We found no significant relationship between N_0 and total incident SW (or average SW, data not shown), although the trend was positive. Relatively constrained fitted values for N_0 (9 % CV) compared to γ (CV 140%) imply that the rate of extinction of N_L with canopy depth is a more variable canopy characteristic across sites than top of canopy N_L. The low variability of N_0 across Arctic sites is surprising given the host of other factors that affect soil N availability such as soil type, depth, moisture and temperature, and presence and absence of permafrost. We argue however that these soil factors are more likely to affect *whole plant*, or *whole canopy* N_T (and L_T) rather than top of canopy N_L. For example, in a global meta-analysis, Poorter *et. al*. (2009) show that whole plant leaf area is more responsive to nutrient limitation than leaf mass per unit area, which is only affected when growth becomes severely limited. The highest N_T values recorded were in grass dominated communities in Svalbard underneath cliffs, perhaps because of nutrient enrichment by sea birds or run off from snow melt from plateaus above.

Predicting L_T from NDVI: the importance of bryophytes

Comparing the relationship between P and L_T required indirect measurements of L_T based on

NDVI. The calibration relationships between L_T and *NDVI* suggests that including information on moss abundance in the high arctic can improve the accuracy of L_T estimates. We found a positive relationship between the % cover of mosses and the NDVI of the ground surface after the vascular canopy had been removed. Including the effect of mosses on background NDVI reduced error in L_T prediction in all cases. This improvement is surprising considering the inaccuracies inherent in visually estimating percent cover, and the probable variability in moss NDVI with water content and species. We deal with only peak growing season data in this study, but we expect that the effect of mosses on NDVI will be greater at the start and end of the growing season, when more of the ground surface is visible from above. The large abundances of mosses at Zackenberg (pers. obs) may also act to increase the impact of structural vegetation properties on the L_T-NDVI relationship (Steltzer *et al.*, 2006), because of the effects of canopy structure on the degree to which underlying mosses are visible from above. This could also simply be because the vascular vegetation was most strongly patchy at Zackenberg, where there were more sites with a high proportion of bare ground. Without including information on moss cover at Zackenberg, NDVI was able to explain only 37 % of the variation in L_T.

The relationship between L_T and P across Arctic latitudes

We found no significant improvement in model fit by including vegetation type in models of P_{1000} and E_0. This is unsurprising as functional convergence of PFTs in Arctic vegetation has previously been reported, and we argue that this is a direct result of the close convergence of the L_T-N_T relationship within a site (Williams *et al.*, 2006, Street *et al.*, 2007, Shaver *et al.*, 2007). We found a significant improvement in the P_{1000} model fit by including site level effects on γp and p_m, though this improvement was small (RMSE was reduced by < 0.2 μmol m^{-2} s^{-1}). The

effects of soil moisture and vapour pressure deficit will also control *P* through effects on stomata conductance (Rastetter *et al.*, 2010) contributing to noise in the relationship between *P* and L_T and masking the effect of site in this simple model. We suggest however that an analysis which takes into account changes in stomatal conductance, might reveal clearer site level differences in the relationship between *P* and L_T.

Implications

We show that, at peak growing season, Arctic plant canopies follow a narrowly-constrained set of rules that dictate the development of leaf area with respect to canopy nitrogen. The way coupling is achieved however, differs between sites – with a trade-off at the canopy scale between canopy leaf N concentration and leaf thickness. The L_T-N_T relationship represents an extremely powerful tool in up-scaling leaf level processes to canopies and ecosystems, by collapsing large amounts of variation in leaf properties within and between species.

The mechanism by which L_T-N_T coupling is achieved is unknown. A study by Campioli *et al.* (2009a) showed that the ratio of canopy L_T:N_T in tundra plant communities is well-constrained through time, from 2 weeks after bud burst to 2 weeks before senescence. This suggests either a 'hard-wired' community composition which results in convergence as soon as leaves emerge, or that the reallocation of N within the canopy responds very rapidly to environmental conditions and developing canopy structure. The next steps are to investigate the mechanisms by which L_T-N_T coupling is achieved and to test whether similar relationships exist not only for Arctic plant canopies, but for plant canopies globally.

We achieved a small improvement in model fit by including site level parameters in the relationship between *P* and L_T. After accounting for variation in stomatal conductance this

improvement could be more significant and warrants further investigation. There may be potential for improvements in regional *P* models that are based on estimates of L_T, through incorporating differences in the L_T-N_T relationship between sites and/or differences in moss cover. Our results suggest that site based differences in the curvature of the L_T-N_T relationship are linked to the average fraction of incident radiation that is diffuse. If this is the case, there is potential for improving carbon models without the need for further data input; canopy N extinction parameters could be adjusted based on average incident radiation conditions.

Our results also imply that predicted increases in cloudiness as a result of Arctic climate change (Vavrus *et al.*, 2009) may result in redistribution of N within canopies and ecosystems. This reallocation could be significant. If for example, we assume that diffuse fraction directly controls the parameter γ, Fig. 2a indicates that for a canopy with an L_T of 1.5 m^2 m^{-2} an increase in average diffuse fraction from roughly 66 % (Toolik) to 80 % (Svalbard) might result in the 'optimal' total foliar nitrogen content doubling; from around 2 to 4 g N m^{-2}. Re-allocation of N on this magnitude would have important implications for other ecosystem processes such as litter decomposition, herbivory, and belowground carbon allocation.

ACKNOWLEDGEMENTS

This work was supported by grants from the US National Science Foundation to the Marine Biological Laboratory including grants # OPP-0352897, DEB-0423385, and DEB-0444592. We thank Jim Laundre at the MBL and the staff at Toolik Field Station and Abisko Scientific Research Station for their help and support. Bob Douma and Celine Ronfort assisted with fieldwork in Sweden and Svalbard. We acknowledge; Glenn Scott from the Arctic Observing Network (AON), US, Siegrid Debatin from the Alfred Wegener Institute Foundation for Polar

and Marine Research, Germany and Jonathan Evans from the Centre of Ecology and Hydrology, UK (through the ABACUS project) for providing radiation data. Dr. Charles N. Long at ARM, US also made radiation data available for us. We also thank Paul Stoy and Adrian Rocha for their valuable comments on a previous version of this manuscript.

REFERENCES

Anten NPR, Hirose T (1999) Interspecific differences in above-ground growth patterns result in spatial and temporal partitioning of light among species in a tall-grass meadow. *Journal of Ecology,* **87,** 583-597.

Anten NPR, Schieving F, Werger MJA (1995) Patterns of Light and Nitrogen Distribution in Relation to Whole Canopy Carbon Gain in C-3 and C-4 Monocotyledonous and Dicotyledonous Species. *Oecologia,* **101,** 504-513.

Baddeley JA, Woodin SJ, Alexander IJ (1994) Effects of Increased Nitrogen and Phosphorus Availability on the Photosynthesis and Nutrient Relations of 3 Arctic Dwarf Shrubs from Svalbard. *Functional Ecology,* **8,** 676-685.

Beer C, Reichstein M, Tomelleri E, *et al.* (2010) Terrestrial Gross Carbon Dioxide Uptake: Global Distribution and Covariation with Climate. *Science,* **329,** 834-838.

Bekryaev RV, Polyakov IV, Alexeev VA (2010) Role of Polar Amplification in Long-Term Surface Air Temperature Variations and Modern Arctic Warming. *Journal of Climate,* **23,** 3888-3906.

Bond BJ, Farnsworth BT, Coulombe RA, Winner WE (1999) Foliage physiology and biochemistry in response to light gradients in conifers with varying shade tolerance. *Oecologia,* **120,** 183-192.

Brown J, Miller PC, Tieszen LL, Bunnell FL (1980) In *US IBP Synthesis Series*, Vol. 12, pp. 571. Dowden, Hutchinson, and Ross, Stroudsburg, PA.

Campioli M, Michelsen A, Samson R, Lemeur R (2009a) Seasonal variability of leaf area index and foliar nitrogen in contrasting dry-mesic tundras. *Botany-Botanique,* **87,** 431-442.

Campioli M, Street LE, Michelsen A, Shaver GR, Maere T, Samson R, Lemeur R (2009b) Determination of Leaf Area Index, Total Foliar N, and Normalized Difference Vegetation Index for Arctic Ecosystems Dominated by Cassiope tetragona. *Arctic Antarctic And Alpine Research,* **41,** 426-433.

Chapin FS, Oechel WC (1983) Photosynthesis, Respiration, and Phosphate Absorption by Carex-Aquatilis Ecotypes Along Latitudinal and Local Environmental Gradients. *Ecology,* **64,** 743-751.

Chapin FS, Shaver GR, Giblin AE, Nadelhoffer KJ, Laundre JA (1995) Responses Of Arctic Tundra To Experimental And Observed Changes In Climate. *Ecology,* **76,** 694-711.

Clark DB, Mercado LM, Sitch S, *et al.* (2011) The Joint UK Land Environment Simulator (JULES), model description - Part 2: Carbon fluxes and vegetation dynamics. *Geoscientific Model Development,* **4,** 701-722.

Collatz GJ, Ribas-Carbo M, Berry JA (1992) Coupled photosynthesis-stomatal conductance model for leaves of C4 plants *Australian Journal of Plant Physiology,* **19,** 519-538.

de Pury DGG, Farquhar GD (1997) Simple scaling of photosynthesis from leaves to canopies without the errors of big-leaf models. *Plant Cell And Environment,* **20,** 537-557.

Erbs DG, Klein SA, Duffie JA (1982) Estimation of the Diffuse-Radiation Fraction for Hourly, Daily and Monthly-Average Global Radiation. *Solar Energy,* **28,** 293-302.

Evans JR (1989) Photosynthesis and Nitrogen Relationships in Leaves of C-3 Plants. *Oecologia,* **78,** 9-19.

Falge E, Baldocchi D, Tenhunen J, *et al.* (2002) Seasonality of ecosystem respiration and gross primary production as derived from FLUXNET measurements. *Agricultural and Forest Meteorology,* **113,** 53-74.

Farquhar GD, Caemmerer SV, Berry JA (1980) A biochemical-model of photosynthetic CO_2 assimilation in leaves of C-3 species. *Planta,* **149,** 78-90.

Field C (1983) Allocating Leaf Nitrogen for the Maximization of Carbon Gain - Leaf Age as a Control on the Allocation Program. *Oecologia,* **56,** 341-347.

Forland EJ, Hanssen-Bauer I (2000) Increased precipitation in the Norwegian Arctic: True or false? *Climatic Change,* **46,** 485-509.

Grant RF, Humphreys ER, Lafleur PM, Dimitrov DD (2011) Ecological controls on net ecosystem productivity of a mesic arctic tundra under current and future climates. *Journal of Geophysical Research-Biogeosciences,* **116**.

Hikosaka K, Hirose T (1997) Leaf angle as a strategy for light competition: Optimal and evolutionarily stable light-extinction coefficient within a leaf canopy. *Ecoscience,* **4,** 501-507.

Hikosaka K, Hirose T (1998) Leaf and canopy photosynthesis of C-3 plants at elevated CO2 in relation to optimal partitioning of nitrogen among photosynthetic components: theoretical prediction. *Ecological Modelling,* **106,** 247-259.

Hill GB, Henry GHR (2011) Responses of High Arctic wet sedge tundra to climate warming since 1980. *Global Change Biology,* **17,** 276-287.

Hirose T (2005) Development of the Monsi-Saeki theory on canopy structure and function. *Annals of Botany,* **95,** 483-494.

Hirose T, Werger MJA (1987) Maximizing Daily Canopy Photosynthesis with Respect to the Leaf Nitrogen Allocation Pattern in the Canopy. *Oecologia,* **72,** 520-526.

Hollister RD, Webber PJ, Bay C (2005) Plant response to temperature in Northern Alaska: Implications for predicting vegetation change. *Ecology,* **86,** 1562-1570.

Leuning R, Kelliher FM, Depury DGG, Schulze ED (1995) Leaf nitrogen, photosynthesis, conductance and transpiration - scaling from leaves to canopies. *Plant Cell And Environment,* **18,** 1183-1200.

Meir P, Kruijt B, Broadmeadow M, *et al.* (2002) Acclimation of photosynthetic capacity to irradiance in tree canopies in relation to leaf nitrogen concentration and leaf mass per unit area. *Plant Cell And Environment,* **25,** 343-357.

Niinemets U (2007) Photosynthesis and resource distribution through plant canopies. *Plant Cell And Environment,* **30,** 1052-1071.

Niinemets U (2010) A review of light interception in plant stands from leaf to canopy in different plant functional types and in species with varying shade tolerance. *Ecological Research,* **25,** 693-714.

Piao SL, Friedlingstein P, Ciais P, Viovy N, Demarty J (2007) Growing season extension and its impact on terrestrial carbon cycle in the Northern Hemisphere over the past 2 decades. *Global Biogeochemical Cycles,* **21**.

Ping CL, Michaelson GJ, Jorgenson MT, Kimble JM, Epstein H, Romanovsky VE, Walker DA (2008) High stocks of soil organic carbon in the North American Arctic region. *Nature Geoscience,* **1,** 615-619.

Rastetter EB, Williams M, Griffin KL, *et al.* (2010) Processing arctic eddy-flux data using a simple carbon-exchange model embedded in the ensemble Kalman filter. *Ecological Applications,* **20,** 1285-1301.

Reich PB, Oleksyn J (2004) Global patterns of plant leaf N and P in relation to temperature and latitude. *Proceedings Of The National Academy Of Sciences Of The United States Of America,* **101,** 11001-11006.

Reichstein M, Ciais P, Papale D, *et al.* (2007) Reduction of ecosystem productivity and respiration during the European summer 2003 climate anomaly: a joint flux tower, remote sensing and modelling analysis. *Global Change Biology,* **13,** 634-651.

Roderick ML, Farquhar GD, Berry SL, Noble IR (2001) On the direct effect of clouds and atmospheric particles on the productivity and structure of vegetation. *Oecologia,* **129,** 21-30.

Ryu Y, Baldocchi DD, Kobayashi H, *et al.* (2011) Integration of MODIS land and atmosphere products with a coupled-process model to estimate gross primary productivity and evapotranspiration from 1 km to global scales. *Global Biogeochemical Cycles,* **25**.

Shaver GR, Chapin FS (1980) Response to Fertilization by Various Plant Growth Forms in an Alaskan tundra: Nutrient accumulation and growth. *Ecology,* **61,** 662-675.

Shaver GR, Chapin FS (1986) Effect of fertilizer on production and biomass of tussock tundra, Alaska, U.S.A. *Arctic And Alpine Research,* **18,** 261-268.

Shaver GR, Chapin FS (1991) Production - Biomass Relationships And Element Cycling In Contrasting Arctic Vegetation Types. *Ecological Monographs,* **61,** 1-31.

Shaver GR, Street LE, Rastetter EB, Van Wijk MT, Williams M (2007) Functional convergence in regulation of net CO2 flux in heterogeneous tundra landscapes in Alaska and Sweden. *Journal of Ecology,* **95,** 802-817.

Shipley B, Lechoweicz MJ, Wright I, Reich PB (2006) Fundamental trade-offs generating the worldwide leaf economics spectrum. *Ecology,* **87,** 535-541.

Sitch S, McGuire AD, Kimball J, *et al.* (2007) Assessing the carbon balance of circumpolar Arctic tundra using remote sensing and process modeling. *Ecological Applications,* **17,** 213-234.

Steltzer H, Welker JM (2006) Modeling the effect of photosynthetic vegetation properties on the NDVI-LAI relationship. *Ecology*, **87,** 2765-2772.

Street LE, Shaver GR, Williams M, Van Wijk MT (2007) What is the relationship between changes in canopy leaf area and changes in photosynthetic CO2 flux in arctic ecosystems? *Journal of Ecology*, **95,** 139-150.

van Wijk MT, Williams M, Shaver GR (2005) Tight coupling between leaf area index and foliage N content in arctic plant communities. *Oecologia*, **142,** 421-427.

Vavrus S, Waliser D, Schweiger A, Francis J (2009) Simulations of 20th and 21st century Arctic cloud amount in the global climate models assessed in the IPCC AR4. *Climate Dynamics*, **33,** 1099-1115.

von Caemmerer S, Farquhar GD (1981) Some relationships between the biochemistry of photosynthesis and the gas-exchange of leaves *Planta*, **153,** 376-387.

Weih M, Karlsson PS (2001) Growth response of Mountain birch to air and soil temperature: is increasing leaf-nitrogen content an acclimation to lower air temperature? *New Phytologist*, **150,** 147-155.

Williams M, Rastetter EB (1999) Vegetation characteristics and primary productivity along an arctic transect: implications for scaling up. *Journal of Ecology*, **87,** 885-898.

Williams M, Street LE, van Wijk MT, Shaver GR (2006) Identifying Differences in Carbon Exchange among Arctic Ecosystem Types. *Ecosystems*, **9,** 288-304.

Wright IJ, Reich PB, Westoby M, *et al.* (2004) The worldwide leaf economics spectrum. *Nature*, **428,** 821-827.

Wylie D, Jackson DL, Menzel WP, Bates JJ (2005) Trends in global cloud cover in two decades of HIRS observations. *Journal of Climate*, **18,** 3021-3031.

Ziehn T, Kattge J, Knorr W, Scholze M (2011) Improving the predictability of global CO(2) assimilation rates under climate change. *Geophysical Research Letters,* **38**.

SUPPORTING INOFORMATION LEGENDS

Fig. S1. Global short wave (SW) vs. photosynthetically active radiation (PPFD) data from Toolik Lake Field station for 12th July to 13th September and 24th October to 26th November 2008

Fig. S2. a) Modelled and measured total daily diffuse radiation through time at a Abisko, June 2008

Fig. S3. a) Modelled and measured total daily diffuse radiation through time at Toolik Lake, for a 8 week period in late summer 2008.

TABLES

Table 1. List of symbols, abbreviations and units

Symbol	Definition	Units
L_T	Leaf area index	m^2 leaf m^{-2} ground
N_T	Total foliar nitrogen per unit ground	g N m^{-2} ground
M_T	Total leaf mass per unit ground	g leaf m^{-2} ground
N_L	Nitrogen per unit leaf area	g N m^{-2} leaf area
N_M	Nitrogen per unit leaf mass	g N g^{-1} leaf mass
L_M	Specific leaf area	m^2 leaf g^{-1} leaf
I	Photosynthetic photon flux density	μmol photons m^{-2} ground s^{-1}
P	Gross primary productivity	μmol CO_2 m^{-2} ground s^{-1}
$NDVI$	Normalised difference vegetation index	unitless
$NDVI_{post}$	NDVI measure after vascular canopy removal	unitless
$NDVI_{min}$	Minimum measured value of $NDVI_{post}$ (= 0.24)	unitless
$NDVI_{max}$	Fitted parameter representing maximum canopy NDVI	unitless
K_c	Fitted extinction coefficient controlling curvature of $NDVI$-L_T calibration	m^2 ground m^{-2} leaf
a	Intercept of relationship between $NDVI_{min}$ and bryophyte cover	unitless
B_c	Slope of relationship between $NDVI_{min}$ and bryophyte cover	$\%^{-1}$
F_c	Net ecosystem exchange	μmol CO_2 m^{-2} ground s^{-1}
R_E	Ecosystem respiration	μmol CO_2 m^{-2} ground s^{-1}
P_{max}	Theoretical light saturated photosynthetic rate	μmol CO_2 m^{-2} ground s^{-1}
E_0	Initial light use efficiency of photosynthesis	μmol CO_2 μmol^{-1} photons
P_{1000}	Gross primary productivity at 600 μmol m^{-2} I	μmol CO_2 m^{-2} ground s^{-1}
γ	Nitrogen extinction coefficient	m^2 ground m^{-2} leaf
N_0	Top of canopy N_L	g N m^{-2} leaf area
γ_p	P extinction coefficient	m^2 ground m^{-2} leaf
P_0	Top of canopy P_{1000} per unit leaf area	μmol CO_2 μmol^{-1} m^{-2} leaf s^{-1}
P_m	Constant representing moss photosynthesis	μmol CO_2 μmol^{-1} m^{-2} s^{-1}
α	Slope of relationship between E_0 and L_T	μmol CO_2 μmol^{-1} photons m^{-2} leaf
E_m	Constant in relationship between E_0 and L_T representing moss P	μmol CO_2 μmol^{-1} photons

Table 2. Summary of data including year, site, number of measurements and literature source.

Data type (plot sizes)	Year	Site	n	Source
harvest (0.03 $m^{2)}$	2009	Barrow, Alaska	23	This study
harvest (0.03 m^2, 0.05 m^2, 0.09 m^2)	2006	Zackenberg, NE Greenland	28, 26, 24	This study
harvest (0.05 m^2)	2005	Longyearbyen, Svalbard	48	This study
harvest (0.04 m^2)	2001	Abisko, Sweden	92	Van Wijk *et al.* (2005)
harvest (0.04 m^2)	1997	Kuparuk watershed, Alaska	94	Williams & Rastetter (1999)
Chamber *P* (1 m^2)	2009	Barrow, Alaska	10	This study
Chamber *P* (1 m^2 , 0.09 m^2)	2006	Zackenberg, NE Greenland	26, 15	This study
Chamber *P* (1 m^2)	2005	Longyearbyen, Svalbard	36	This study
Chamber *P* (1 m^2)	2004	Toolik Lake, Alaska	28	Shaver *et al.* (2007) & Street *et al.* (2007)
Chamber *P* (1 m^2)	2004	Abisko, Sweden	45	Shaver *et al.* (2007)

Table 3. Average specific leaf area (L_M), leaf nitrogen per unit leaf area (N_L) and leaf nitrogen per unit leaf mass (N_M) for plant species at Svalbard, Zackenberg and Barrow. Species for which n < 5 are not included. Plant functional types (PFT) are: D = deciduous, E = evergreen, F = forb, G = graminoid.

Site	Species	n	PFT	N_L [g m^{-2}]	N_M [mg g^{-1}]	L_M [m^2 kg^{-1}]
Barrow	*Salix phlebophylla*	7	D	1.76 ± 0.09	23.3 ± 1.8	13.2 ± 0.3
	Stellaria species	9	F	1.43 ± 0.17	22.4 ± 1.6	17.4 ± 2.2
	Saxifraga cernua	8	F	0.95 ± 0.07	19.4 ± 1.3	20.6 ± 1.0
	Dupontia fisheri	15	G	2.21 ± 0.17	23.1 ± 1.0	11.2 ± 0.8
	Eriophorum scheuchzeri	10	G	2.51 ± 0.23	30.3 ± 1.9	12.5 ± 0.6
	other grasses	9	G	1.73 ± 0.14	19.3 ± 1.0	11.5 ± 0.6
Svalbard	*Salix polaris*	34	D	1.75 ± 0.05	24.2 ± 0.8	13.9 ± 0.4
	Dryas octopetala	21	E	2.68 ± 0.13	20.2 ± 0.6	8.1 ± 0.8
	Cassiope tetragona	6	E	2.16 ± 0.20	19.8 ± 1.2	4.6 ± 0.2
	Polygonum viviparum	35	F	2.06 ± 0.07	30.8 ± 0.3	15.5 ± 0.5
	other forbs	20	F	1.88 ± 0.20	24.9 ± 1.1	15.1 ± 1.3
	Equisetum species	30	P	3.14 ± 0.18	28.4 ± 1.3	9.5 ± 0.5
	Carex species	9	G	1.90 ± 0.17	19.3 ± 1.3	10.6 ± 0.9
	Dupontia fisheri	5	G	2.09 ± 0.20	16.1 ± 1.3	7.8 ± 0.2
	other graminoids	32	G	2.32 ± 0.10	21.6 ± 0.6	9.7 ± 0.3
Zackenberg	*Salix arctica*	58	D	2.18 ± 0.08	30.9 ± 1.0	14.4 ± 0.6
	Arctostaphylos alpina	14	D	2.87 ± 0.20	31.1 ± 2.0	11.1 ± 0.6
	Vaccinium uliginosum	14	D	1.44 ± 0.05	24.6 ± 1.3	16.2 ± 1.5
	Dryas species	23	E	2.12 ± 0.09	16.0 ± 0.7	8.0 ± 0.5
	Cassiope tetragona	22	E	2.15 ± 0.19	23.2 ± 0.6	5.8 ± 0.4
	Polygonum viviparum	37	F	4.01 ± 1.09	38.3 ± 1.0	15.9 ± 1.3
	Stellaria species	16	F	2.15 ± 0.57	27.0 ± 1.5	17.6 ± 1.9
	Pedicularis species	8	F	2.40 ± 0.23	36.2 ± 3.7	16.1 ± 2.5
	Equisetum species	12	P	2.62 ± 0.10	27.3 ± 1.9	10.4 ± 0.5
	Carex species	8	G	2.17 ± 0.22	24.9 ± 1.9	11.8 ± 0.8
	Dupontia species	6	G	2.45 ± 0.21	21.3 ± 2.7	8.6 ± 0.7
	Eriophorum species	6	G	2.47 ± 0.12	25.9 ± 1.6	10.7 ± 0.9
	other graminoids	28	G	4.47 ± 2.03	24.9 ± 1.4	11.1 ± 1.1
	other grasses	18	G	5.07 ± 1.69	28.6 ± 1.6	8.2 ± 0.9
	other sedges	5	G	2.25 ± 0.26	24.9 ± 2.1	11.5 ± 1.2

Table 4. Model description and structure, Akaike's information criteria (AIC), Bayes Information Criteria (BIC), logliklihood (LogLik) and root mean square error (RMSE) for alternative N_T models (equation 4) describing the data shown in Figure 2a. Parameters are fitted either for the whole data set, or separately for each site or PFT. " - " indicates that grouping factors for site or PFT are not included i.e. there is a single fitted value of the parameter for the whole data set.

N_T model description	**Grouping structure**		**Number of parameters**	**AIC**	**BIC**	**LogLik**	**RMSE [g N m^{-2} ground]**
	N_0	γ					
No site or PFT effect	-	-	3	5.9	21.0	1.06^{*+}	0.27
Site effects (on N_0 and γ)	**Site**	**Site**	**15**	**-201.3**	**-140.9**	**$153.1^{+\&£}$**	**0.18**
Site effects (on N_0 only)	Site	-	11	-171.4	-129.1	$97.7^{\&}$	0.23
Site effects (on γ only)	-	Site	11	-180.9	-135.5	$102.4^{£}$	0.19
PFT effects (on N_0 and γ)	PFT	PFT	15	-86.2	-25.7	59.1^{*}	0.25

£ & $ * + matching symbols indicates pairs of nested models where the log likelihood ratio test is significant at 0.05 level.

Table 5. Model description and structure, Akaike's information criteria (AIC), Bayes Information Criterion (BIC), loglikelihood (LogLik) and root mean square error (RMSE) for alternative P_{1000} models (equation 6) describing the data displayed in Figure 6a. Parameters are fitted either for the whole data set, or separately for each site/PFT " - " indicates that no grouping factors are included in the model for that parameter i.e. there is a single fitted value of the parameter for the whole data set.

P_{1000} model description	**Grouping structure**			**Number of parameters**	**AIC**	**BIC**	**LogLik**	**RMSE [μmol m^{-2} s^{-1}]**
	P_0	γ_p	P_m					
No site or PFT effect	-	-	-	4	356.9	369.2	-173.4$^{*\$+}$	1.89
Site effects (on P_0 and γ_p)	Site	Site	-	12	354.3	386.1	-164.1*	1.73
Site effects (on γ_p and P_m)	-	**Site**	**Site**	**12**	**353.8**	**385.8**	**-163.9**$^{\$\#\wedge}$	**1.71**
Site effects (on P_m only)	-	-	Site	8	355.2	377.3	-168.6$^{+\wedge}$	1.81
Site effects (on γ_p only)	-	Site	-	8	358.9	381.0	-170.5$^{\#}$	1.81
Site effects (on P_0 only)	Site	-	-	8	357.8	379.9	-169.9	1.81
PFT effects (on P_0 and γ_p)	PFT	PFT	-	10	360.5	387.5	-169.2	1.77
PFT effects (on γ_p and P_m)	-	PFT	PFT	10	358.1	385.1	-168.0	1.78

Pairs of matching symbols (* $ + # ^) indicates nested models where the log likelihood ratio test is significant at 0.05 level. For all light curves maximum I exceeded 1000 μmol m^{-2} s^{-1}

Table 6. Model structure, Akaike's information criteria (AIC), Bayes information criterion (BIC), loglikelihood (LogLik) and the root mean square error (RMSE) for alternative E_0 models (equation 7) describing the data displayed in Figure 6b. Parameters are fitted either for the whole data set, or separately for each site/PFT. " - " indicates that no grouping factors are included in the model for that parameter. i.e. there is a single fitted value of the parameter for the whole data set

E_0 model description	**Grouping structure**		**Number of parameters**	**AIC**	**BIC**	**LogLik**	**RMSE [μmol m^{-2} s^{-1}]**
	α	E_m					
No site or PFT effect	**-**	**-**	**3**	**-638.2**	**-628.4**	**323.1**	**0.0060**
Site effects (on α and E_m)	Site	Site	11	-628.6	-599.2	326.3	0.0057
Site effects (on α only)	-	Site	7	-631.7	-612.1	323.9	0.0059
Site effects (on E_m only)	Site	-	7	-632.6	-612.9	324.3	0.0060
PFT effects (on α and E_m)	PFT	PFT	9	-630.9	-606.4	325.5	0.0058

For all light curves maximum I exceeded 600 μmol m^{-2} s^{-1}

FIGURES

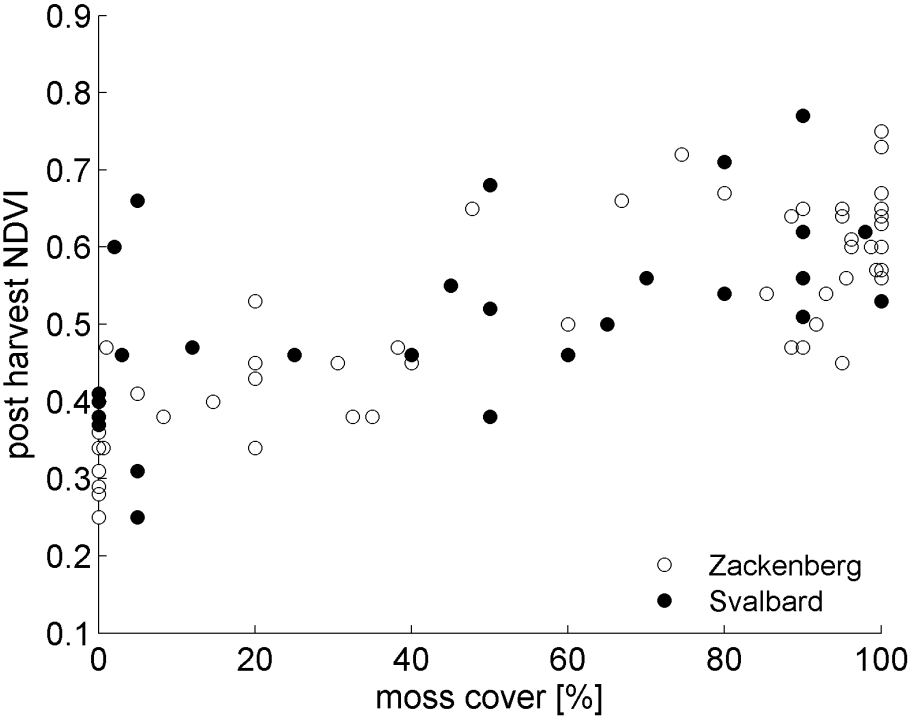

Figure 1. Post harvest NDVI ($NDVI_{post}$) and percent moss cover (*B*c) for Zackenberg and Svalbard.

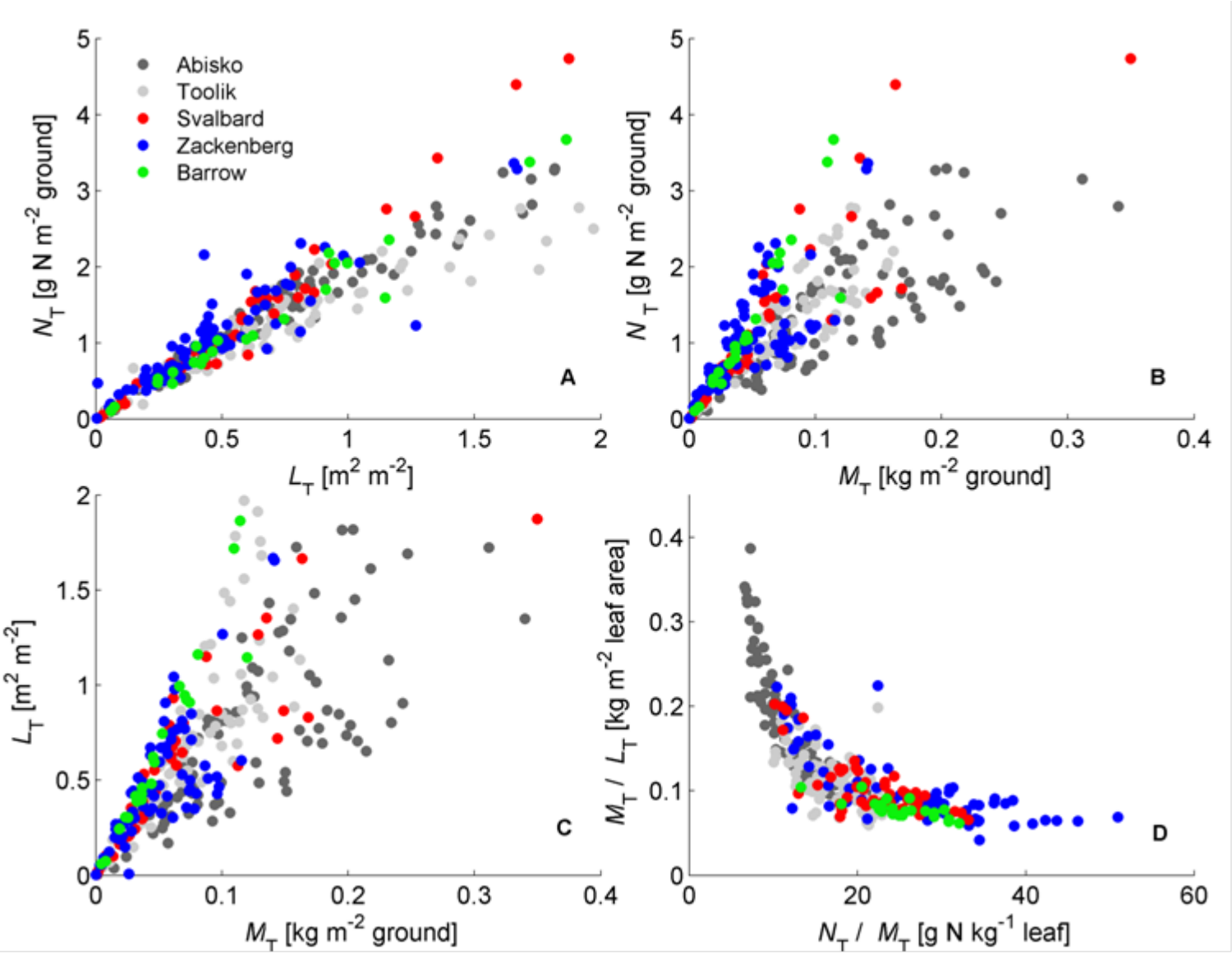

Figure. 2. Inter-comparison of relationships between a) N_T and L_T b) N_T and M_T c) L_T and M_T and d) M_T/L_T and N_T/M_T for vegetation harvests at Svalbard 2005 (n = 49), Abisko 2002 (n = 92) and Toolik 1997 (n = 94), Zackenberg (n = 78) and Barrow (n = 23).

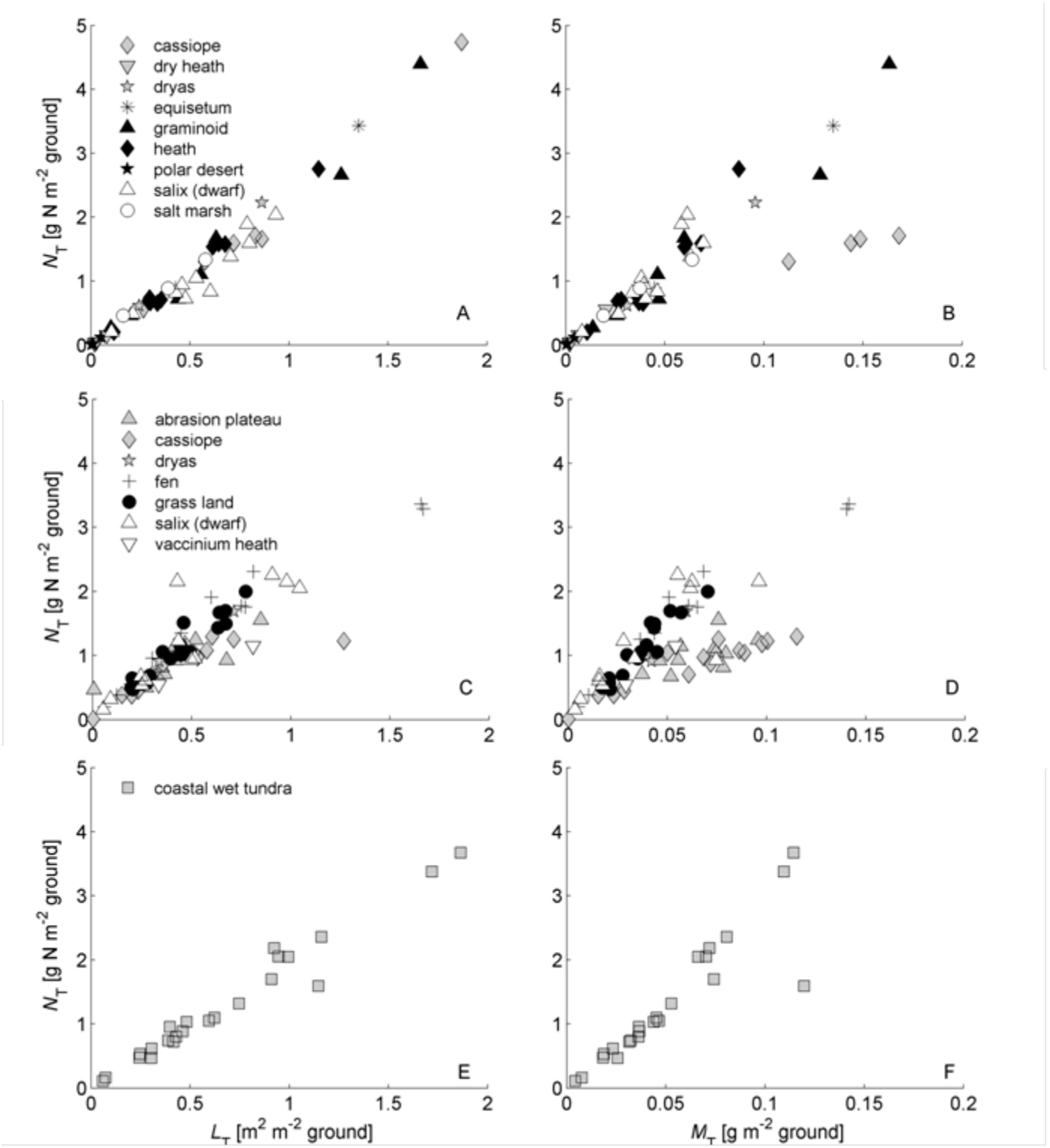

Figure 3. Relationships between N_T and L_T (left panels) and N_T and M_T (right panels) for vegetation harvests in **a,b**) Svalbard 2005 (n = 49), **c,d**) Zackenberg 2006 (n = 78) and **e,f**) Barrow 2009 (n = 23). Data points classified by vegetation type.

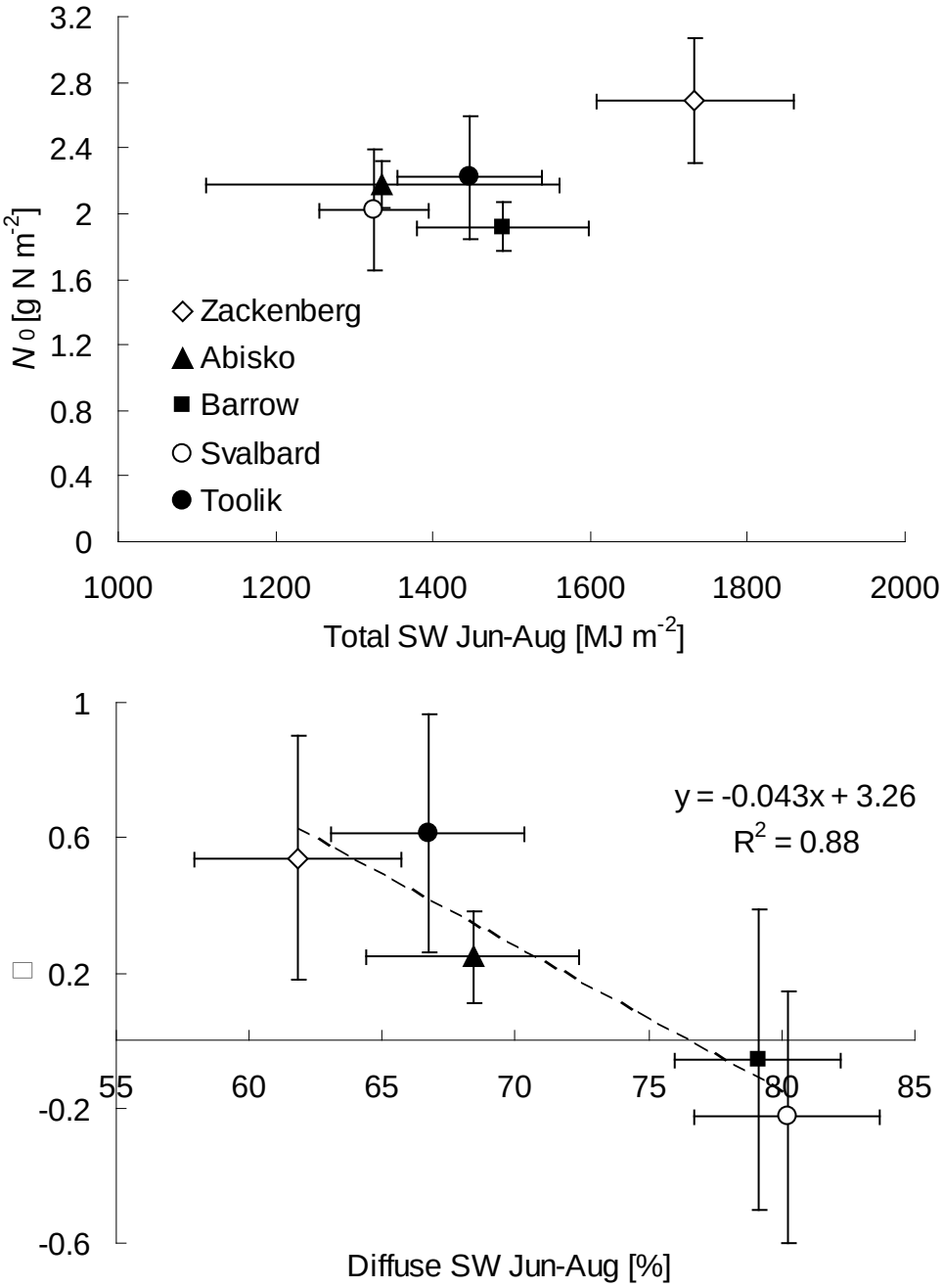

Figure 4 Site-specific fitted values of **a)** N_0 vs. total growing season short wave radiation and **b)** γ versus diffuse radiation fraction for Abisko, Barrow, Toolik, Svalbard and Zackenberg. Horizontal error bars are standard deviation for 5 years of radiation data. Vertical error bars are 90 % confidence interval for fitted parameters.

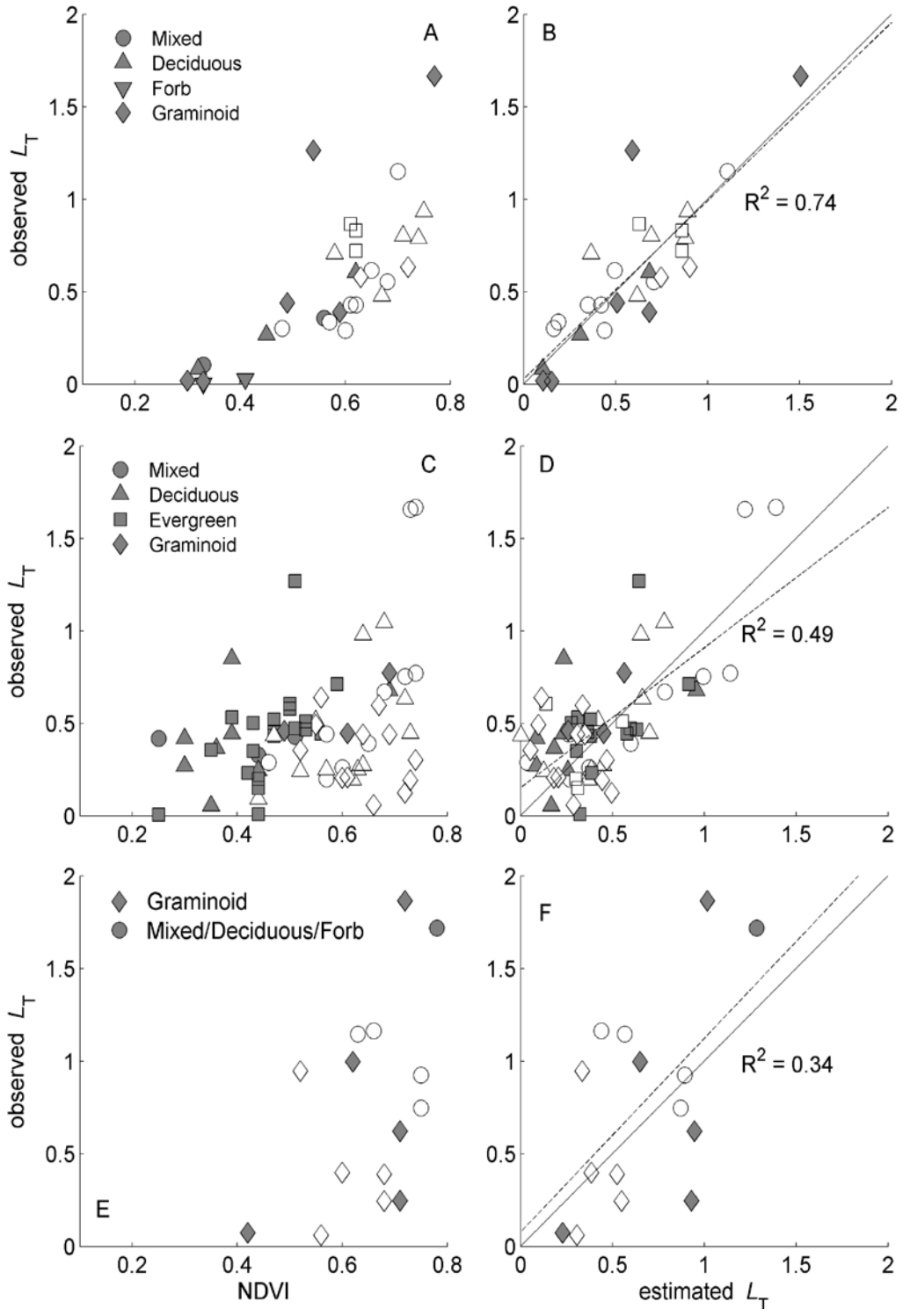

Figure 5 The relationship between NDVI and L_T for the destructively harvested plots (left panels) and between modelled and measured L_T for the same plots, based on equation 2 fitted separately for each plant functional type (right panels) **a,b)** Svalbard, **c,d)** Zackenberg and **e,f)** Barrow. Open sysmbols show plots where moss cover is > 50 %, filled symbols show plots where moss cover < 50 %.

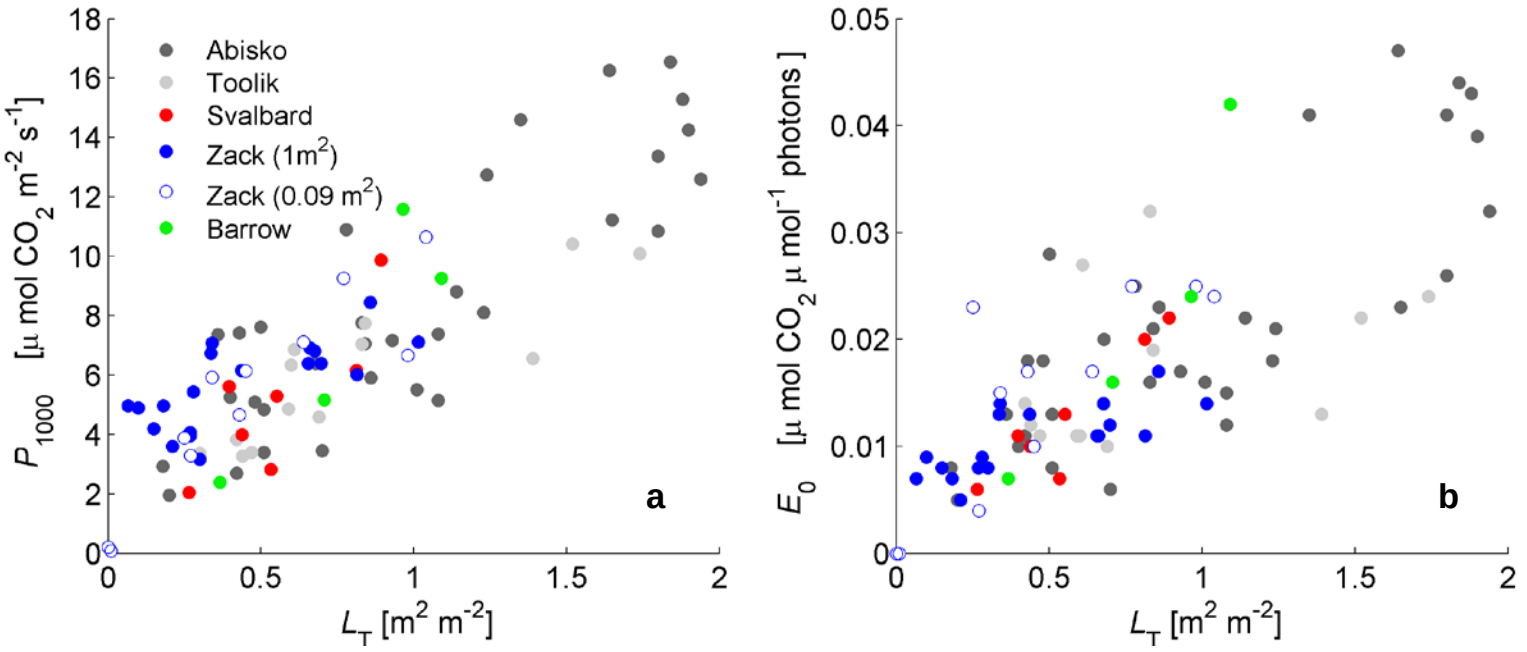

Figure 6 a) The relationship between P_{1000} and L_T and **b)** E_0 and L_T for Svalbard, Abisko Toolik, Zackenberg and Barrow.

SUPPORTING INFORMATION

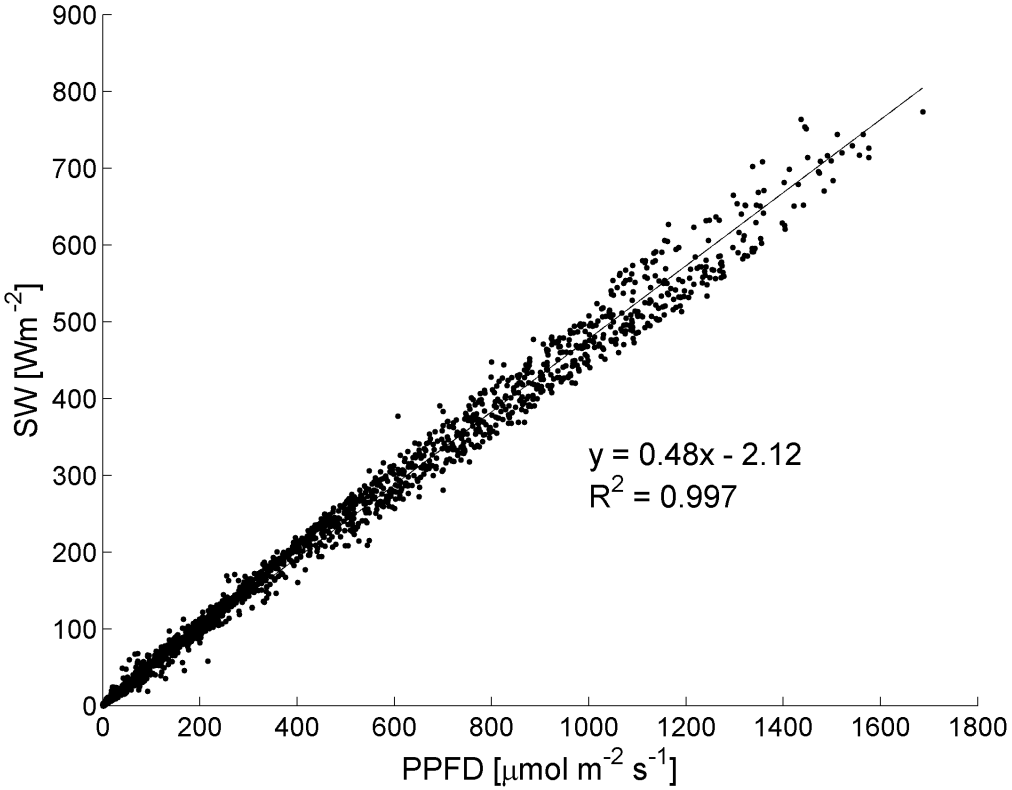

Fig. S1. Global short wave (SW) vs. photosynthetically active radiation (PPFD) data from Toolik Lake Field station for 12th July to 13th September and 24th October to 26th November 2008

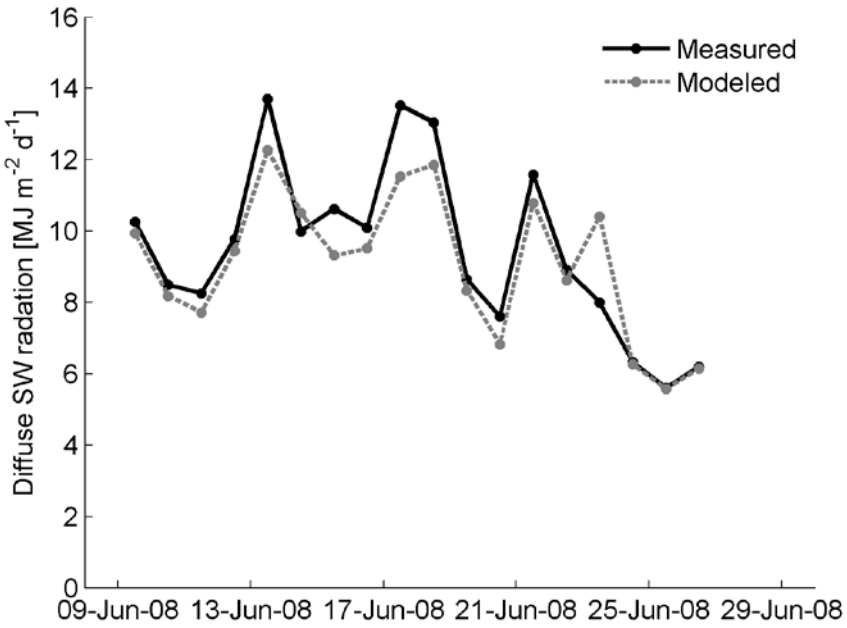

Fig. S2. a) Modelled and measured total daily diffuse radiation through time at a Abisko, June 2008

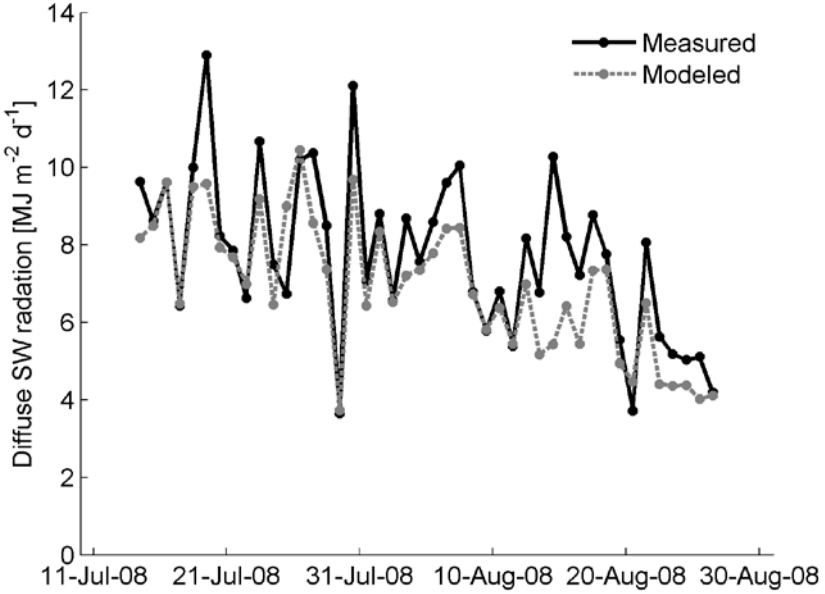

Fig. S3. a) Modelled and measured total daily diffuse radiation through time at Toolik Lake, for a 8 week period in late summer 2008.